# Experimental and petrological investigations into the origin of the lunar Chang'e 5 basalts

Haupt C P*, Renggli C J, Klaver M, Steenstra E S, Berndt J, Rohrbach A, Klemme S,

[1] Institut für Mineralogie, Universität Münster, Münster, 48149, Deutschland

*Corresponding author: chaupt1@uni-muenster.de

ORCID: 0000-0003-1932-9677

## Abstract

The origin of young Chang'e 5 (CE5) lunar basalts is highly debated. We present results from high-pressure, high-temperature (*P*-*T*) phase equilibria experiments, and from petrological modeling, to constrain the depth and temperature of the source of these unique mare basalts. The experimental results indicate that the CE5 basalts could have formed either by melting clinopyroxene and Fe-Ti oxide-rich cumulates in the shallow lunar mantle, or by extreme fractional crystallization of a hot Mg-rich parental melt. Our findings corroborate the local preservation of significant heat (of at least 1200 °C) in the lunar mantle that is needed to generate basaltic melts of CE5 compositions at 2 Ga. We argue that the CE5 basalts are most likely formed by melting of Fe and Ti-rich cumulates in the shallow lunar mantle as extreme fractional crystallization of olivine and plagioclase from picritic parental melts requires too high temperatures in the lunar mantle (> 1500 °C) at ~2 Ga.



Keywords: lunar mantle, fractional crystallization, lunar basalts, sample recovery mission, experimental petrology


## 1 Introduction

Recently, the Chinese CE5 mission (Che et al., 2021; Qian et al., 2021) returned new basaltic lunar rocks from the Oceanus Procellarum on the Moon. Geochemical studies on these samples, which were sampled in the young mare basalt unit Em4 in the Mons Rümker region (Qian et al., 2018), confirm the young age of these rocks (1.96–2.01 Ga, Che et al., 2021) that had already been dated by crater counting chronology (Hiesinger et al., 2003). This makes the CE5 samples the youngest studied igneous rocks from the Moon, about 1 Ga younger than the basalts from the US Apollo and Soviet Luna missions, and also all lunar basaltic meteorites (Elardo et al., 2014; Shearer et al., 2006). Therefore, the CE5 samples provide an excellent opportunity to study the evolution of the Moon through time.

To explain young lunar volcanism in the Procellarum KREEP (**K**-**REE**-**P**hosphorous) Terrain (PKT) on the Moon, several possible heat sources or melting mechanisms have been suggested, which include a lunar source that is rich in the KREEP (last remaining liquid after crystallization of the lunar magma ocean also enriched heat-producing elements like U and Th) or water (Borg et al., 2004; Laneuville et al., 2013; McCubbin et al., 2010). However, the CE5 basalts do not show a typical geochemical signature of that component (Tian et al., 2021), and the hypothesis that young lunar basalts originated from a KREEP-rich mantle source (e.g., Borg et al., 2004; Laneuville et al., 2013) appears highly unlikely. Moreover, the CE5 samples contain little water and other volatiles (Hu et al., 2021; Liu et al., 2022). Ziethe et al. (2009) proposed an insulating layer of megaregolith, which reduced heat loss from the lunar mantle and hence extended the duration of volcanic activity. In contrast, a thin crust (<30 km; Wieczorek et al., 2013) in the PKT region could lead to adiabatic decompression melting and enable volcanism in that area late in the lunar history (Tian et al., 2021).

In this study we investigate the origin of the CE5 basalts using a two-fold approach. First, we conducted high-pressure, high-temperature experiments to ascertain if the CE5 basalts could be primary, unfractionated melts that have formed by melting of a lunar mantle cumulate.

Multiple saturation point (MSP) experiments as conducted in this study have proven useful to unravel the origin of primitive lunar basalt samples such as picritic pyroclastic glasses (Chen et al., 1982; Green et al., 1971, 1975; Hughes et al., 1988). These primitive samples (e.g., very low titanium A14 and A17 volcanic glasses; Chen et al., 1982; A17 orange glass; Green et al., 1975) are multiply saturated with olivine (Ol) and orthopyroxene (Opx) on their liquidus at ~2.0–2.5 GPa and ~1400–1500 °C. These findings indicate that the picritic glasses represent near-primary basaltic melts derived from a mantle source that consists of olivine and orthopyroxene within the lunar interior at depths greater than 400 km.

Second, we modeled the fractional crystallization of different primitive parental melt compositions to establish, if the CE5 basalts could have formed by extensive fractionation of magmatic mineral phases such as

olivine and plagioclase. The CE5 basalts cannot be primary melts from an olivine-rich lunar mantle, since low MgO/MgO+FeO (Mg# = 0.27) usually indicate extensive fractionation of olivine and/or pyroxenes (Borg et al., 2004; Che et al., 2021; Papike and Vaniman, 1978). Indeed, this is the preliminary interpretation for the origin of the CE5 samples presented recently (Che et al., 2021; Tian et al., 2021). To further our understanding of the evolution of the lunar mantle, and the generation of the Chang'e 5 basalts, we present new experiments and fractional crystallization modeling.

# 2 Methods

### 2.1. Starting material compositions

Two starting materials were prepared to match the bulk composition of CE5-B1 and CE5-B2 basalt fragments (Che et al., 2021). These starting materials were synthesized by mixing reagent grade oxides and carbonates ($SiO_2$, $Al_2O_3$, $TiO_2$, MgO, $Cr_2O_3$, $CaCO_3$, $MnCO_3$, $K_2CO_3$, $Na_2CO_3$). Magnesium oxide was fired at 1000 °C to remove hydroxide or carbonate, and the resulting MgO was always kept in a drying oven at 110 °C. The starting materials were homogenized in an agate mortar for 40 min under ethanol and the mixtures were dried, placed in a Pt-crucible and decarbonated in a box furnace at 1000 °C for 10 h, followed by another 40 min of grinding and mixing. Iron was then added to the decarbonated mixture as hematite ($Fe_2O_3$) and P as $H_9N_2O_4P$. The resulting Fe- and P-bearing mixtures were fused in a Pt-crucible at 1350 °C, reground and reduced in graphite containers at 1100 °C in a vertical gas-mixing furnace (Gero GmbH, Germany) for 12 h, using a steady flow of CO gas to impose an $fO_2$ corresponding to the graphite-CO-buffer and the final starting material contained only $Fe^{2+}$.

The starting materials were always stored in a desiccator. To measure the starting material composition, ~15 mg of the starting material was mounted on Re-wire loops and fused in a vertical gas-mixing furnace at the iron-wüstite buffer (IW) and 1350 °C. The resulting glasses were embedded in epoxy resin, polished and carbon coated for electron microprobe analysis. The chemical compositions of the starting materials together with the lunar CE5 basalt compositions are shown in Table 1.

*Table 1. Chemical compositions of CE5 basalts CE5-B1 and B2 and the experimental starting materials*

| | Chang'e 5 basalts | | Experimental starting materials | |
|---|---|---|---|---|
| Chemical composition (wt.%) | CE5-B1 | CE5-B2 | BE-1 (n=10) | BE-2 (n=10) |
| $SiO_2$ | 39.46–44.04 | 38.17–45.57 | 40.6(1) | 43.0(2) |
| $TiO_2$ | 4.37–7.91 | 5.84–9.68 | 5.7(2) | 7.8(2) |
| $Al_2O_3$ | 9.77–13.51 | 4.44–8.08 | 11.0(1) | 7.03(7) |
| FeO | 17.51–27.69 | 19.42–29.58 | 24.5(2) | 22.7(1) |
| MnO | 0.2–0.38 | 0.25–0.41 | 0.29(2) | 0.38(2) |
| MgO | 3.07–5.91 | 3.12–7.22 | 4.51(5) | 5.45(7) |
| CaO | 7.15–13.61 | 10.13–13.17 | 11.7(1) | 12.23(9) |
| $Na_2O$ | 0.17–0.51 | 0.16–0.36 | 0.38(5) | 0.35(5) |
| $K_2O$ | 0–0.19 | 0–0.18 | 0.11(2) | 0.15(2) |
| $Cr_2O_3$ | 0.03–0.25 | 0.05–0.19 | 0.37(5) | 0.27(2) |
| $P_2O_5$ | 0.06–0.36 | 0.08–0.26 | 0.19(4) | 0.23(3) |
| Total | | | 99.3(9) | 99.5(8) |

*The compositions experimental starting materials BE-1 and BE-2 determined using Electron Microprobe (EPMA) with 1 σ standard deviations given in brackets and reported as last digits, e.g. 0.19(4) should read as 0.19 ±0.04 wt.%, n = number of analyses*

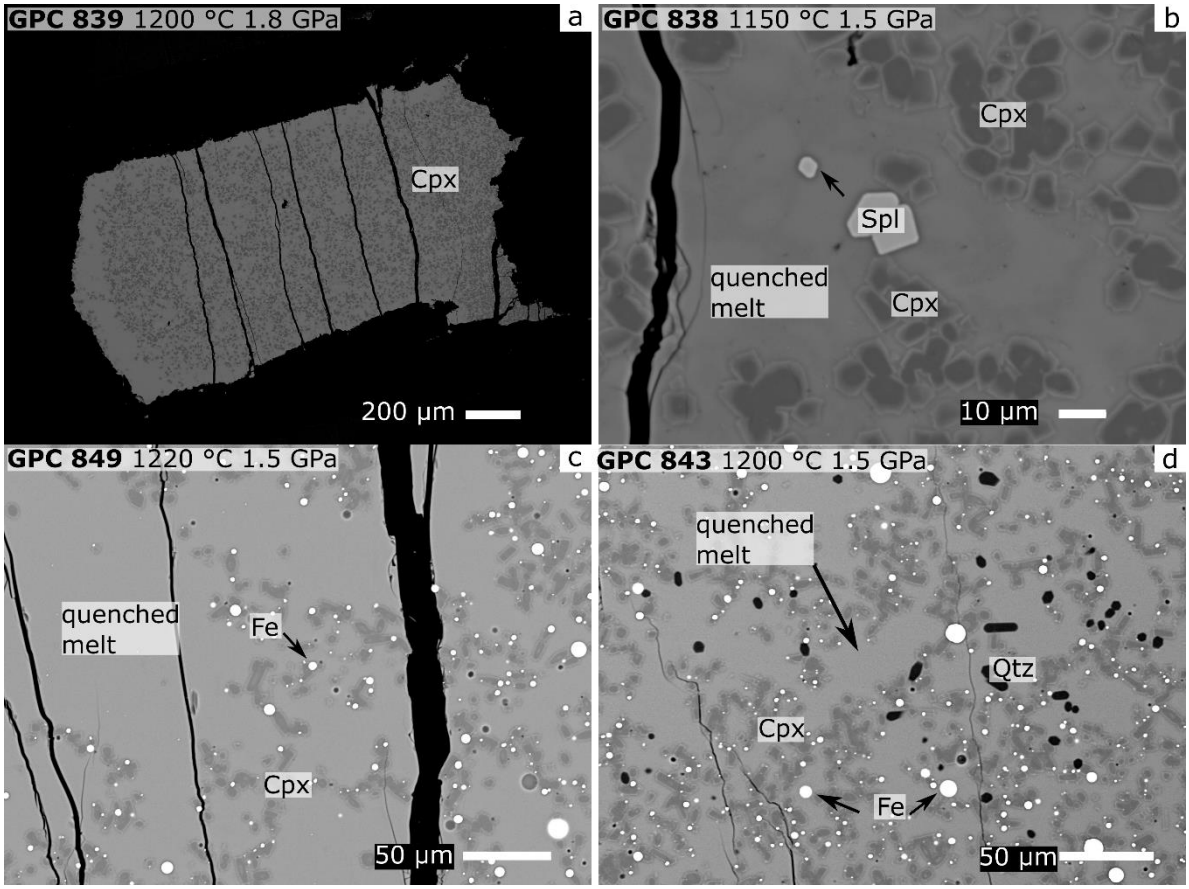


*Figure 1 Back-scattered electron (BSE) images of the run products from BE-1 (a–b) and BE-2 (c–d) starting materials compositions. (a) Run GPC 839 containing quenched melt and clinopyroxene (Cpx) at 1.8 GPa and 1200 °C. (b) Run GPC 838 contains quenched melt, clinopyroxene and traces of spinel (spl) (c) run GPC 849 contains quenched melt, clinopyroxene and Fe-metal blebs (d) Run GPC 843 contains small (<20 µm) euhedral quartz grains (Qtz), clinopyroxene, Fe-blebs and quenched melt*

### 2.2 Multiple saturation point (MSP) experiments

The experiments between 1 and 2.5 GPa were performed in an end-loaded piston-cylinder apparatus (Boyd and England, 1960). The starting materials were loaded into graphite capsules that were placed into ½ inch

piston-cylinder assemblies that consist of inner cylinders made of crushable alumina (6 mm outer diameter), surrounded by a straight graphite furnace, a Duran glass cylinder (Schott, GmbH) and an outer talk sleeve. The assembly was calibrated using the quartz-coesite transition (Bose and Ganguly, 1995) and the $MgCr_2O_4$ + $SiO_2$= $MgSiO_3$ + $Cr_2O_3$ reaction (Klemme and O'Neill, 1997) and resulted in a friction correction of –13 %. Based on our pressure calibration, the quoted pressures are accurate within 0.07 GPa. Experimental run temperatures were monitored and controlled using a W-Re-thermocouple (Type D) and an Eurotherm controller (Schneider Electric, Germany). Experiments were quenched by shutting off the electrical power. The experimental conditions and results are given in Table 2 and exemplary back-scattered electron images, taken with a scanning electron microscope, of the run products are shown in Figure 1.

*Table 2. Experimental results of high-pressure piston cylinder (PC) experiments on compositions BE-1 and BE-2.*

| Run No. | Starting material | T [°C] | P [GPa] | Duration [hrs] | Phases | Modal proportions | Sum of sq. residuals |
|---|---|---|---|---|---|---|---|
| GPC 834 | BE-1 | 1100 | 1 | 17 | Cpx, FeTiOx+Ilm, Pl | 64:13:23 | 1.352 |
| GPC 841 | BE-1 | 1130 | 1 | 17 | Cpx, FeTiOx, Pl, melt | 22:2:8:68 | 0.055 |
| GPC 838 | BE-1 | 1150 | 1.5 | 14 | Cpx, FeTiOx, melt | 17:<1:82 | 0.19 |
| GPC 831 | BE-1 | 1180 | 1 | 8 | FeTiOx, melt | <1:99 | 0.76 |
| GPC 844 | BE-1 | 1200 | 1.5 | 8.5 | Cpx, melt | 10:90 | 0.125 |
| GPC 839 | BE-1 | 1200 | 1.8 | 7 | Cpx, melt | 16:84 | 0.23 |
| GPC 827 | BE-1 | 1250 | 1 | 14 | melt (+ Fe) | 99:<1 | 0.136 |
| GPC 837 | BE-1 | 1300 | 2.5 | 6 | melt | 100 | 0.144 |
| GPC 853 | BE-1 | 1180 | 1.4 | 8.5 | Cpx, melt | 10:90 | 1.4 |
| GPC 856 | BE-1 | 1180 | 1.2 | 8.5 | FeTiOx, melt | <1:99 | 0.497 |
| GPC 862 | BE-1 | 1160 | 1.3 | 9 | FeTiOx, Cpx, melt | <1:17:82 | 1.09 |
| GPC 863 | BE-2 | 1180 | 1.2 | 8 | Fe-metal, Cpx, Qtz, melt | 12:18:1:69 | 1.2 |
| GPC 842 | BE-2 | 1150 | 1 | 17 | Fe-metal, Qtz, Cpx, | 10:6:37: 7:7:<1:33 | 0.03 |

| | | | | | | | |
|---|---|---|---|---|---|---|---|
| | | | | | Ilm, Pl, Ttn, melt | | |
| GPC 843 | BE-2 | 1200 | 1.5 | 8 | Fe-metal, Qtz, Cpx, melt | 12:1:18:69 | 0.21 |
| GPC 848 | BE-2 | 1200 | 1 | 10 | Fe-metal, Cpx, melt | 11:4:85 | 0.39 |
| GPC 849 | BE-2 | 1220 | 1.5 | 7 | Fe-metal, Cpx, melt | 12:10:78 | 0.713 |
| GPC 851 | BE-2 | 1250 | 1 | 8.5 | Fe-metal, melt | 13:87 | 0.134 |

*Phase proportions determined by least squares linear regression of analyzed phases (Supplementary Material) per run against starting composition. Phase abbreviations: clinopyroxene = Cpx, plagioclase = Pl, quartz = Qtz, titanite = Ttn, Fe-Ti-oxides (FeTiOx) comprising ulvöspinel-chromite-spinel solid solutions, and ilmenite (Ilm) , Fe= metallic iron, melt = quenched melt(see also the Supplementary Material), T= temperature in °C, P = pressure in GPa. Modal proportions were calculated using the bulk compositions and mineral compositions.*

All experimental run products were mounted in epoxy-resin and polished using different diamond pastes. The mounts were then carbon coated, examined with a JEOL JSM 6510-LV scanning electron microscope and analyzed quantitatively with an electron probe microanalyzer (EPMA; JEOL JXA 8530 F Hyperprobe) at the Institute for Mineralogy, University of Münster (Germany).

### 2.3 Electron Probe Microanalyses (EPMA)

All EPMA measurements were performed using an acceleration voltage of 15 kV and a beam current of 15 nA except for plagioclase (Pl), which was measured with a beam current of 10 nA. The beam diameters for glass analyses were set according to the size of the melt pockets in the experiments which range from 5 to 20 µm. Silicate and oxide minerals were measured with a beam diameter of 1–5 µm. The matrix corrections were made according to the φ(ρz) procedure (Armstrong, 1991). Details can be found in the Supplementary Material.

### 2.4 Attainment of equilibrium and assessment of $fO_2$ in the experiments

The durations of the experiments (7–17 h) was sufficient to produce compositionally homogeneous minerals (Singletary and Grove, 2008; van Orman and Grove, 2000). Minerals in our runs are small and generally unzoned; only clinopyroxene contains small quench rims (Fig. 1b–d). The standard deviations of the average compositions of mineral and melts are very low, which is consistent with the attainment of chemical equilibrium in these runs. A profile through a large (80 µm) clinopyroxene grain confirms homogeneity (Supplementary Material Fig. 1).

The $fO_2$ for runs on BE-1 was determined in run GPC 831 by adding an Fe-Ir alloy $fO_2$-sensor (resulting in IW+2). We assume that the $fO_2$ is identical in all runs on that composition. All experiments with BE-2 contain Fe-blebs, which indicate a lower $fO_2$ (Sato et al., 1973). The $fO_2$ for BE-2 was estimated using the equilibrium of $2Fe + O_2 = 2FeO$ and resulted in IW–1.5 (for details refer to the supplementary material). The $fO_2$ observed in the experiments is consistent with the current best estimates on $fO_2$ derived from lunar basalt samples (Sato et al., 1973; Wadhwa, 2008). Since run conditions and experimental methods are very similar, we attribute the difference in $fO_2$ between experiments conducted on BE-1 and BE-2 to the different chemical compositions of the starting materials BE-1 and BE-2.

## 3 Results

#### 3. MSP experiments

We performed 17 PC-experiments on starting materials BE-1 and BE-2, representing the CE5 basalts CE5-B1 and CE5-B2 from Che et al. (2021), and exemplary BSE images of the runs are shown in Fig. 1. Table 2 gives the experimental run conditions, stable mineral phases, and calculated phase proportions in each run. More details are given in the Supplementary Material. The high-pressure phase relations for the two compositions are shown in Fig. 2. For composition BE-1, clinopyroxene (Cpx) is the only liquidus phase between 1.4–1.7 GPa and 1180–1200 °C (Fig. 1a; Fig. 2a), and at lower pressures clinopyroxene, plagioclase, Fe-Ti oxides (ulvöspinel-chromite-hercynite-spinel), and ilmenite appear. Fe-Ti oxides are found in some high temperature, low pressure runs (GPC 838, 831, 856; Table 2). As the position of the MSP can only be bracketed by our

experiments, we infer a MSP at pressures between 1.2 and 1.4 GPa, and at temperatures between 1200 and 1250 °C, whereas melts are saturated in both, clinopyroxene and Fe-Ti oxides.

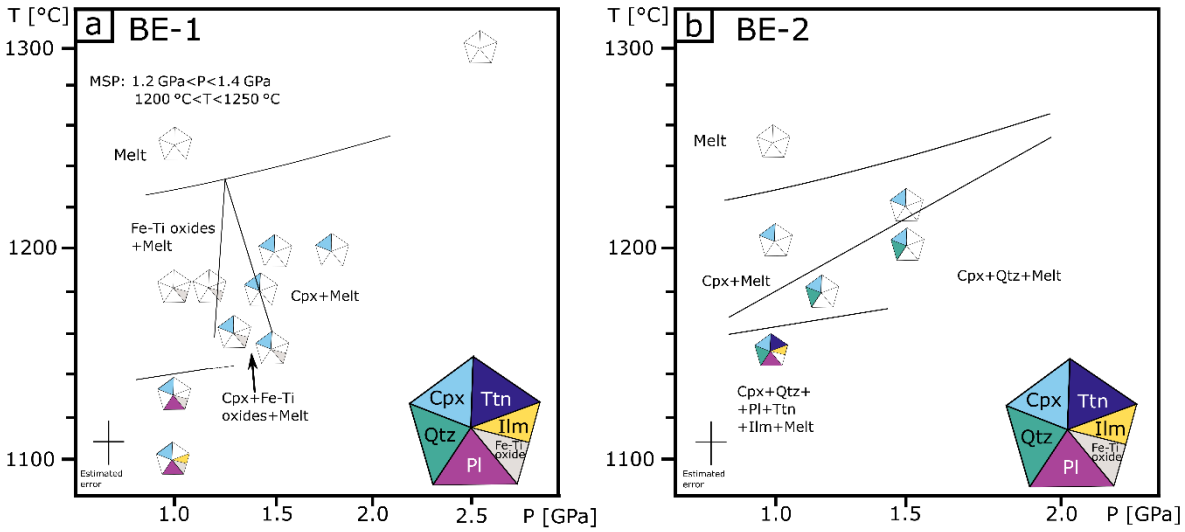


*Figure 2 Pressure-temperature diagram showing the experimental results on the starting materials BE-1 (CE5-B1) (a) and BE-2 (CE5-B2) (b) between 1–2.5 GPa and 1100–1300 °C. Stable mineral phases are depicted in pentagons at the individual P-T conditions: clinopyroxene (Cpx), Fe-Ti oxides (solid solutions of the ulvöspinel-chromite-hercynite-spinel series)), quartz (Qtz), plagioclase (Pl), titanite (Ttn), and ilmenite (Ilm). (a) BE-1 is multiple saturated with clinopyroxene, and Fe-Ti oxides at about 1.3 ±0.1 GPa and 1225±25 °C. (b) BE-2 has only Cpx on the liquidus between 1200–1250 °C and 1–1.5 GPa, but 40–50 °C below the liquidus, Qtz appears at 1.5 GPa and followed by Pl, Ilm, and Ttn at 1 GPa and T = 1180 °C. Note the estimated uncertainties in P and T indicated in (a) and (b).*

Experimental results for the BE-2 starting material are significantly different, as in these runs (Fig. 1c–d, Fig. 2b, Table 2) only clinopyroxene occurs as a liquidus phase (liquidus at 1–1.5 GPa and 1200–1220 °C, Fig. 1c), followed by quartz at 1.5 GPa and 1200 °C (Fig. 1d). Clinopyroxene, quartz, plagioclase, and ilmenite crystallize at 1 GPa and 1150 °C. We conclude that no clear-cut multiply saturated phase assemblage exists for the BE-2 composition, but it should be noted that multiple phase saturation occurs only ca. 40 °C below the liquidus. Furthermore, some runs with BE-1 composition contain sub-micron sized Fe-rich metal grains, which are not significantly affecting mass balance. In contrast, the experiments on CE5-B2 composition contain considerable Fe-metal blebs in all of the experiments (Fig. 1c–d, Table 2; Supplementary Material).

# 4 Discussion

### 4.1. Can the Chang'e 5 basalts be primary melts from Fe- and Ti-rich cumulates?

Our experimental results on the synthetic analog of CE5-B1 show that the system is saturated on the liquidus with clinopyroxene, and Fe-Ti oxides at a pressure of 1.3±0.1 GPa and 1225±25 °C with plagioclase appearing shortly after (~1150 °C; Fig. 1a). The crystallization of either ilmenite or Ti-bearing spinel (Ulvöspinel) as a Fe-Ti-bearing oxide depends on $fO_2$ (Schmitt and Kraettli, 2022). Since both are present in our experiments, we infer a MSP of clinopyroxene and FeTi-oxides. In contrast to most previous studies on lunar samples defining multiple phase saturation, neither orthopyroxene, nor olivine are present in our experiments. The mineral assemblage at multiple phase saturation of the CE5-B1 basalt is also significantly different from most other picritic lunar basalts, which contain olivine, spinel and low-Ca pyroxene at the MSP (Elardo et al., 2015; Green et al., 1975; Grove and Vaniman, 1978). The multiple saturation points for primitive (lunar and terrestrial) basalts must be regarded as minimum pressures and temperatures of origin (e.g., Longhi, 1992a). If the CE5 basalts are primary, unfractionated melts, the MSP indicates that the melt was in equilibrium with clinopyroxene, and Fe-Ti oxides at ~250 km depth within the lunar mantle, following the pressure-depth relationship of Elkins-Tanton et al. (2011). This is in stark contrast to the lunar picrites which originated from harzburgite rocks much deeper in the lunar mantle, i.e. at 1.5–2.5 GPa and 1400–1500 °C (Chen et al., 1982; Hughes et al., 1988; Wagner and Grove, 1997), which corresponds to a depth of 300–600 km. A mantle cumulate from which the CE5 basalts originated has to be of different character. Our experiments show that the CE5-B1 basalt might be a primary melt from a late stage cumulate containing clinopyroxene and Fe-Ti oxides. The pressure indicated by our experiments (~1.2 GPa) locates these cumulate at a depth of at least 250 km within the lunar mantle, which supports that the late stage cumulates did not persist at their original depth of ~100 km (Snyder et al., 1992), but sank further into the mantle, as proposed by the overturn hypothesis (e.g., Green et al., 1975; Spera, 1992; Ringwood and Kesson, 1976; van Orman and Grove, 2000; Wagner and Grove, 1997).

Our MSP is further supported by experimental investigations on near-liquidus phase relations of high-Ti, high-Fe cumulates yielding very similar phase assemblages with first clinopyroxene and clinopyroxene + Fe-Ti oxides crystallizing between 1100–1200 °C at 0–1.3 GPa. Additionally, the coexisting melt

compositions are similarly enriched in FeO and depleted in MgO (van Orman and Grove, 2000). Even the appearance of quartz is reported in these experiments, which we find in the experiments on the CE5-B2 experimental analogue. Experiments with the CE5-B2 composition (i.e., BE-2), however, do not show a MSP (Fig. 2b). Nevertheless, the near-liquidus phases are similar to composition B1 and we conclude, that the former composition is not far from being multiple saturated. According to the petrographic evaluation of both natural CE5 samples (Che et al., 2021 Electronic Supplementary Material), B1 seems to be the less-altered sample and, according to its major element composition, is generally more representative for the young Em4 unit, sampled during the ChangE5 mission (Li et al., 2022). Thus, we regard the MSP found for B1 composition as most significant for the CE5 basalts.

### 4.2. Are the Chang'e 5 basalts products of extensive fractional crystallization from picritic parental melts?

The experimental evidence for CE5 basalts being primary melts of a shallow source (~250 km) is only one of the hypotheses discussed in recent studies (e.g., Zhong et al., 2022). Based on the high FeO content (~23 wt.% FeO) and low Mg# (~0.27), several studies propose that these basalts are not primary melts, but the product of extensive fractional crystallization (Che et al., 2021; Tian et al., 2021). For example, Tian et al. (2021) suggested low-degree (2–3 %) partial melting from a harzburgite mantle followed by extensive (43–78 %) fractional crystallization as a possible scenario.

To critically evaluate our experimental findings, we explore here if fractional crystallization can be a way to produce the CE5 basalts, and if we can make any reasonable assumptions about the composition of the potential parental magma of these basalts. Specifically, we tested whether the CE5 basalts can be derived from lunar picritic melts (A14yellow, A17orange A15red: Delano, 1986; A17yellow: Delano and Lindsley, 1983; A15yellow: Hughes et al., 1988). These samples, tiny glass beads in the lunar soils, are of volcanic origin and likely pristine samples of the lunar interior (Delano, 1986) and hence, may be good candidates for parental melts of the CE5 basalts. We chose the most primitive glasses, according to their MgO. These primitive

compositions were experimentally proven to be melts that originate from the deep lunar interior (Krawczynski and Grove, 2012; Brown and Grove, 2015). The description of the fractional crystallization model and the normalized major element compositions of these glasses are listed in the Electronic supplementary material.

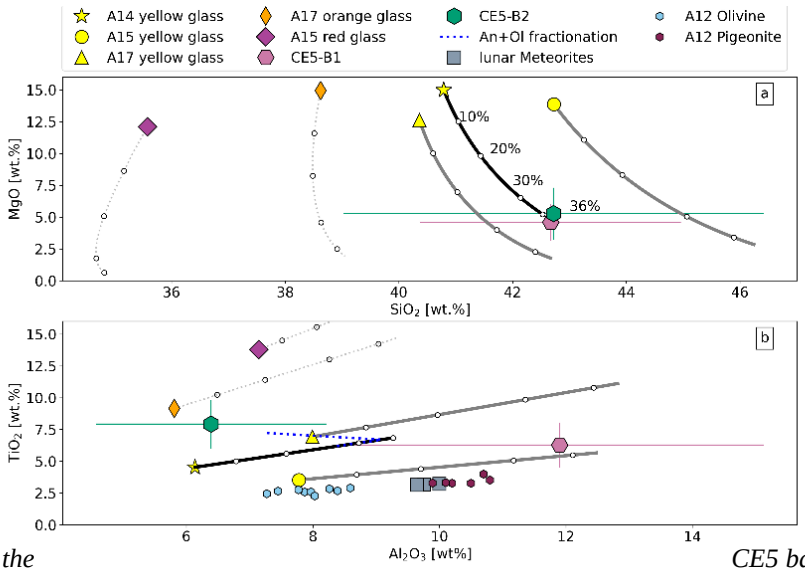


*Figure 3. Variation diagrams showing the liquid line of descent of possible parental melt compositions upon fractional crystallization of equilibrium olivine (Ol) and anorthite (b, blue dotted line). Also given are the two CE5 basalt compositions CE5-B1 and CE5-B2 (hexagons) (a) MgO vs $SiO_2$: Ol fractionation only (grey lines) of primary Apollo glass melts. The results show that the A17 orange and A14 red glass compositions cannot be parental melts of the CE5 basalts, but fractional crystallization of olivine from the yellow glass melt compositions lead to the CE5 basalts (within the uncertainties) (b)$TiO_2$ vs $Al_2O_3$: Ol only fractionation of a A14 yellow glass parental melt leads to a melt that is (just) within the uncertainties of the CE5-B1 composition, but additional fractionation of plagioclase (blue stippled line) is needed to move the $Al_2O_3$ of the fractionating melt composition towards the compositional range of the CE5-B2 sample. Additional information added are A12 Ol basalts (blue hexagons), A12 Pigeonite (Pig) basalts (purple hexagons), and lunar basaltic meteorites NWA4734, 032 and LAP02205 (all together referred to as lunar meteorites; grey squares; plotted compositions taken from Elardo et al. 2014 and Day et al. 2006 and references therein). Natural samples fall on the Ol fractionation trendline from yellow picritic glasses towards CE5 basalts. A15 yellow glass, lunar meteorites and A12 basalts appear to have fractionated from a similar source (Elardo et al., 2015)*

Melt evolution trends are caused by olivine and minor plagioclase fractional crystallization (Fig. 3; Longhi, 1992b; Rhodes et al., 1977). As shown in Fig. 3 (a), the fractional crystallization of olivine alone (grey solid lines) from primitive parental melts lead towards lower MgO in the evolved melts. However, the orange glass composition and the red glass composition are not suitable candidates for parental melts of the CE5 basalts (Fig. 3). Fractional crystallization of olivine from parental melt with yellow glass composition (A14, A15, and A17) yields a melt composition that is within the range of the CE5 samples (Fig. 3, Electronic Supplementary

Fig. 2). The modeling outcome for both investigated CE5 compositions, however, is slightly different. The fractional crystallization path in Figure 3 shows, that about 36±8 % Ol crystallization from a parental melt with primitive A14 yellow glass composition can leads to a melt composition within the range of the CE5-B1. On the other hand, to move the fractionation line closer to the low-alumina composition CE5-B2, which is not achieved in the $TiO_2$-$Al_2O_3$ space by the fractionation of olivine alone (Fig. 3b), additional fractionation of plagioclase together with olivine (blue dotted line Fig. 3b) is required. Specifically, that includes initial 33 % olivine fractionation followed by 8±4 % olivine and plagioclase fractionation to shift the melt composition towards the CE5-B2 (depicted as the blue stippled line in Fig. 3b). Our suggestion for additional plagioclase fractionation is supported by the fact that plagioclase can appear after olivine fractionation towards ambient pressures (Elardo et al., 2015; Grove and Vaniman, 1978) in low-Ti mare basalts. We argue, that CE5-B2 composition could have experienced a slightly faster near-surface cooling to initiate plagioclase crystallization. The $TiO_2$ contents of both CE5 compositions lie within the liquid composition of a fractionated parental melt of A14 yellow glass composition after ~36 % olivine fractionation. (Fig. 3b). In order to produce Fe enriched, Mg depleted young lunar basalts, olivine fractionation from a primitive parental mantle source seems to be a viable process (e.g., Elardo et al., 2015). The CE5 basalts could be products of olivine fractionation from a primitive source - a similar processes potentially responsible for the genesis of the ~1 Ga older lunar meteorite samples (LAP02205, NWA4734, NWA032; compiled major element compositions in Elardo et al., 2015) and the A12 low-Ti basalts (Fig. 3b).

### 4.3. On the thermal state of the lunar mantle at the time of CE5 basalt generation

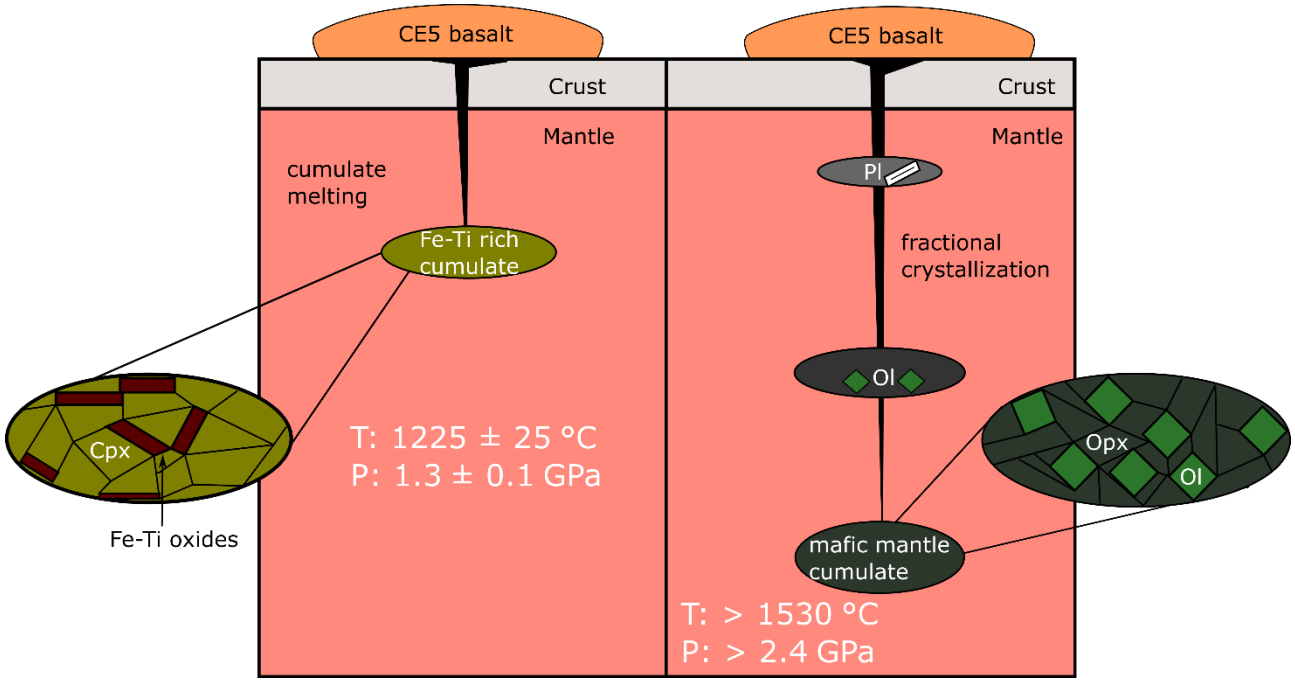


235

236 *Figure 4 Diagrams showing hypothesis (a) and (b) of the origin of young CE5 lunar basalts at 2 Ga. (a)*
237 *According to the experimental results, the CE5 basalts are the result of melting of a late stage mantle cumulate (Fe-Ti*
238 *rich cumulate) consisting of clinopyroxene (Cpx) and Fe-Ti oxides at T 1225±25 °C at a depth of ~250 km. (b) Fractional*
239 *crystallization of olivine (Ol) and minor fractions of plagioclase (Pl) from a primitive melt of a harzburgite lunar mantle*
240 *cumulate (P and T taken from MSP experiments of Brown and Grove, 2015). A14 yellow glass, the potential parental*
241 *melt of CE5 basalts, is at multiple saturation with orthopyroxene (Opx) and olivine (Ol) at ~500 km depth and 1530 °C,*
242 *the conditions where the melt would have started its fractionation path to the lunar surface, if the CE5 samples would be*
243 *product of fractional crystallization.*

244

245 In the previous sections we have introduced two possible scenarios that can explain the origin of the young
246 CE5 basalts.
247 First, experimental results provide constraints that the CE5 basalts could have originated as melts from a late
248 stage mantle cumulate with a MSP at 1.3±0.1 GPa and 1225±25 °C (Fig. 4a). Second, the CE5 basalts can
249 alternatively be explained as the product of extensive fractional crystallization from a primitive picritic melt
250 with a composition similar to the A14 yellow glass (Fig. 4b). Here, we discuss which of these models is more
251 favorable based on the current understanding we have about the thermal evolution of the lunar mantle.

If we consider the experimentally determined conditions of multiple phase saturation of the CE5 samples as the minimum depth and temperature of origin, where they were last in equilibrium with a mantle melt, the young CE5 basalts would have originated from a depth of at least 250 km within the lunar mantle and at temperatures of at least 1200 °C. This would be an extraordinarily high temperature within the lunar mantle at this time, as conventional symmetric lunar thermal evolution models (Spohn et al., 2001; Ziethe et al., 2009) predict much lower temperatures at 250 km depths at 2 Ga (~800–850 °C), under no circumstances hot enough to cause mantle melting. Significant retention of internal heat in the Moon is predicted by thermal models which include a combination of an insulating layer of megaregolith (i.e., Ziethe et al., 2009), a crustal thickness of about 35 km and the highest concentration of heat producing elements in the mantle. The optimum conditions for mantle melting in the relevant depth of ~250 km, however, do not persist until ~2 Ga, the time of CE5 basalt generation (Ziethe et al., 2009).

More recent lunar thermal evolution models, that consider an asymmetric chemical composition of the lunar mantle and crust with an elevated concentration of heat producing elements (KREEP+U, Th) in the mantle right below the crust in the PKT region, lead to an asymmetric thermal evolution of the lunar mantle and localized higher temperatures on the lunar nearside (Laneuville et al., 2013, 2018; Zhang et al., 2022). The highest melt production at depths of 600 km depth starts at 4.5 Ga with a peak between 4–3.5 Ga ceasing at 0.2 Ga within the PKT region (Laneuville et al., 2013). Similarly, the model of Laneuville et al. (2018) predicts volcanic activity on the lunar nearside until ~2 Ga, given enhanced heat production in the mantle beneath the PKT. Generally, these models still tend to overestimate melt volume and underestimate the period of volcanic activity on the Moon.

Given the experimentally determined minimum P (1.3±0.1 GPa) and T conditions (1225±25 °C) of melting of the lunar mantle for CE5 basalt formation, we find that such an asymmetric thermal evolution of the lunar interior is a prerequisite for prolonged volcanic activity on the lunar nearside (Laneuville et al., 2013, 2018; Zhang et al., 2022). This asymmetry can potentially be linked to the South Pole-Aitken basin (SPA) impact (Zhang et al., 2022). This giant impact would have caused a thermochemical instability which pushed

the lunar mantle cumulates and the associated KREEP material towards the lunar nearside (Zhang et al., 2022) and hence, caused or amplified a lunar magma ocean overturn (Ringwood and Kesson, 1976; Snyder et al., 1992). The dynamic mixing and secondary melting due to concentration of heat-producing elements might have formed a heterogeneous source necessary for the long-lasting period of mare volcanism (Laneuville et al., 2013, 2018; Zhong et al., 2000). However, the impact dates back to 4.2–4 Ga and thus cannot be the direct heat source for melting of Fe- and Ti-rich cumulates that must have formed the young CE5 basalts. The young CE5 basalts testify that mantle melting happened at ~2 Ga. Yet, the absence of significant KREEP signatures in the CE5 samples (e.g., Tian et al., 2021) demand for another explanation, then purely KREEP involvement in the source. The distribution of this KREEP component in the lunar mantle, whatever its exact nature may be, has to be very heterogeneous (Borg et al., 2009).

In conclusion, we state that the CE5 basalts could be primary melts of a heterogeneous late stage mantle cumulate, but only if the thermal state of the lunar interior is highly asymmetric leading to a lunar mantle with much less heat loss than in a symmetric lunar mantle. Note, however, that current asymmetric thermodynamic evolution models of the Moon still fail to explain the long-lasting volcanic activity up until ~ 1 Ga and more work is clearly needed on these matters (Laneuville et al. 2013, 2018).

Second, our fractional crystallization model defines a potential source composition of the CE5 basalts with minimum melting conditions of >1500 °C and 2.8–2.5 GPa (Brown and Grove, 2015; Fig. 4), Corresponding to a depth of some 500 km deep within the lunar mantle. If the CE5 basalts were products of fractional crystallization, as proposed by e.g. Tian et al. (2021), the mantle at 500 km depth must have had a temperature of at least 1530 °C around the formation age (~2.0 Ga) of the parental melts of the CE5 basalts (Fig. 4). Based on the discussion of the thermal evolution (see above), it is highly unlikely that a lunar mantle retained such high temperatures (> 1500 °C) until 2 Ga; Ziethe et al., 2009; Laneuville et al., 2013, 2018).

In summary, it is unlikely that the CE5 basalts formed by fractional crystallization from a primitive melt similar to the A14 yellow glass composition, since temperatures of >1500 °C in the lunar mantle at the time of CE5 basalt formation are beyond any thermodynamic assumption (Fig. 4b). Lunar mantle temperatures

of >1200 °C, as indicated by our MSP experiments, are much more likely in the lunar shallow mantle at, or close to the time of eruption of the CE5 basalts at 2 Ga, and hence, we argue that these rocks are most likely product of melting of late-stage, Fe- and Ti-rich cumulates (Fig. 4a).

## Acknowledgements

Our thanks go to Maik Trogisch for his excellent sample preparation and to Beate Schmitte for her superb help with the EPMA measurements. This work was funded by the Deutsche Forschungsgemeinschaft (DFG, German Research Foundation)–Project ID 263649064–TRR 170. This is publication number xxx. MK acknowledges a postdoctoral research fellowship from the Humboldt Foundation. We would also like to thank Clive Neal and an anonymous reviewer for their constructive and very helpful reviews.

# References


Armstrong, J.T., 1991. Quantitative elemental analysis of individual microparticles with electron beam instruments, in: Electron Probe Quantitation. Springer, pp. 261–315.

Borg, L.E., Gaffney, A.M., Shearer, C.K., DePaolo, D.J., Hutcheon, I.D., Owens, T.L., Ramon, E., Brennecka, G., 2009. Mechanisms for incompatible-element enrichment on the Moon deduced from the lunar basaltic meteorite Northwest Africa 032. Geochim. Cosmochim. Acta 73, 3963–3980. https://doi.org/10.1016/j.gca.2009.03.039

Borg, L.E., Shearer, C.K., Asmerom, Y., Papike, J.J., 2004. Prolonged KREEP magmatism on the Moon indicated by the youngest dated lunar igneous rock. Nature 432, 209–211. https://doi.org/10.1038/nature03070

Bose, K., Ganguly, J., 1995. Quartz-coesite transition revisited: reversed experimental determination at 500–1200 C and retrieved thermochemical properties. Am. Mineral. 80, 231–238.

Boyd, F.R., England, J.L., 1960. Apparatus for phase-equilibrium measurements at pressures up to 50 kilobars and temperatures up to 1750°C. J. Geophys. Res. 1896-1977 65, 741–748. https://doi.org/10.1029/JZ065i002p00741.

Brown, S.M., Grove, T.L., 2015. Origin of the Apollo 14, 15, and 17 yellow ultramafic glasses by mixing of deep cumulate remelts. Geochim. Cosmochim. Acta 171, 201–215. https://doi.org/10.1016/j.gca.2015.09.001

Che, X., Nemchin, A., Liu, D., Long, T., Wang, C., Norman, M.D., Joy, K.H., Tartese, R., Head, J., Jolliff, B., Snape, J.F., Neal, C.R., Whitehouse, M.J., Crow, C., Benedix, G., Jourdan, F., Yang, Z., Yang, C., Liu, J., Xie, S., Bao, Z., Fan, R., Li, D., Li, Z., Webb, S.G., 2021. Age and composition of young basalts on the Moon, measured from samples returned by Chang'e-5. Science 374, 887–890. https://doi.org/10.1126/science.abl7957

Chen, H.-K., Delano, J.W., Lindsley, D.H., 1982. Chemistry and phase relations of VLT volcanic glasses from Apollo 14 and Apollo 17. J. Geophys. Res. Solid Earth 87, A171–A181. https://doi.org/10.1029/JB087iS01p0A171

Day, J.M.D., Taylor, L.A., Floss, C., Patchen, A.D., Schnare, D.W., Pearson, D.G., 2006. Comparative petrology, geochemistry, and petrogenesis of evolved, low-Ti lunar mare basalt meteorites from the LaPaz Icefield, Antarctica. Geochim. Cosmochim. Acta 70, 1581–1600. https://doi.org/10.1016/j.gca.2005.11.015

Delano, J.W., 1986. Pristine lunar glasses: criteria, data, and implications. J. Geophys. Res. Solid Earth 91, 201–213. https://doi.org/10.1029/JB091iB04p0D201

Delano, J.W., Lindsley, D.H., 1983. Mare glasses from Apollo 17: constraints on the Moon's bulk composition. J. Geophys. Res. Solid Earth 88, B3–B16. https://doi.org/10.1029/JB088iS01p000B3

Elardo, S.M., Shearer, C.K., Fagan, A.L., Borg, L.E., Gaffney, A.M., Burger, P.V., Neal, C.R., Fernandes, V.A., McCubbin, F.M., 2014. The origin of young mare basalts inferred from lunar meteorites Northwest Africa 4734, 032, and LaPaz Icefield 02205. Meteorit. Planet. Sci. 49, 261–291. https://doi.org/10.1111/maps.12239

Elardo, S.M., Shearer, C.K., Vander Kaaden, K.E., McCubbin, F.M., Bell, A.S., 2015. Petrogenesis of primitive and evolved basalts in a cooling Moon: experimental constraints from the youngest known lunar magmas. Earth Planet. Sci. Lett. 422, 126–137. https://doi.org/10.1016/j.epsl.2015.04.014

Elkins-Tanton, L.T., Burgess, S., Yin, Q.-Z., 2011. The lunar magma ocean: reconciling the solidification process with lunar petrology and geochronology. Earth Planet. Sci. Lett. 304, 326–336. https://doi.org/10.1016/j.epsl.2011.02.004

Green, D.H., Ringwood, A.E., Hibberson, W.O., Ware, N.G., 1975. Experimental petrology of Apollo 17 mare basalts, in: Lunar and Planetary Science Conference Proceedings. pp. 871–893.

Green, D.H., Ringwood, A.E., Ware, N.G., Hibberson, W.O., Major, A., Kiss, E., 1971. Experimental petrology and petrogenesis of Apollo 12 basalts, in: Lunar and Planetary Science Conference Proceedings. p. 601.

Grove, T.L., Vaniman, D.T., 1978. Experimental petrology of very low TI/VLT/basalts, in: Mare Crisium: The View from Luna 24. pp. 445–471.
Hiesinger, H., Head III, J.W., Wolf, U., Jaumann, R., Neukum, G., 2003. Ages and stratigraphy of mare basalts in Oceanus Procellarum, Mare Nubium, Mare Cognitum, and Mare Insularum. J. Geophys. Res. Planets 108. https://doi.org/10.1029/2002JE001985
Hu, S., He, Huicun, Ji, J., Lin, Y., Hui, H., Anand, M., Tartèse, R., Yan, Y., Hao, J., Li, R., Gu, L., Guo, Q., He, Huaiyu, Ouyang, Z., 2021. A dry lunar mantle reservoir for young mare basalts of Chang'E-5. Nature 1–8. https://doi.org/10.1038/s41586-021-04107-9
Hughes, S.S., Delano, J.W., Schmitt, R.A., 1988. Apollo 15 yellow-brown volcanic glass: chemistry and petrogenetic relations to green volcanic glass and olivine-normative mare basalts. Geochim. Cosmochim. Acta 52, 2379–2391. https://doi.org/10.1016/0016-7037(88)90295-5
Klemme, S., O'Neill, H.S., 1997. The reaction MgCr 2 O 4+ SiO 2= Cr 2 O 3+ MgSiO 3 and the free energy of formation of magnesiochromite (MgCr 2 O 4). Contrib. Mineral. Petrol. 130, 59–65.
Krawczynski, M.J., Grove, T.L., 2012. Experimental investigation of the influence of oxygen fugacity on the source depths for high titanium lunar ultramafic magmas. Geochim. Cosmochim. Acta 79, 1–19. https://doi.org/10.1016/j.gca.2011.10.043
Laneuville, M., Wieczorek, M.A., Breuer, D., Tosi, N., 2013. Asymmetric thermal evolution of the Moon. J. Geophys. Res. Planets 118, 1435–1452. https://doi.org/10.1002/jgre.20103
Laneuville, M., Taylor, J., & Wieczorek, M. A., 2018. Distribution of radioactive heat sources and thermal history of the Moon. J. Geophys. Res. Planets, 123, 3144-3166.
Li, C., Hu, H., Yang M.-F., Pei, Z.-Y., Zhou, Q., Ren, X., Liu, B., Zeng, X., Zhang, G., Zhang, H., et al., 2022. Characteristics of the lunar samples returned by the Chang'E-5 mission. Natl. Sci. Rev., 9, nwab188.
Liu, X., Hao, J., Li, R., He, Y., Tian, H., Hu, S., Li, J., Gu, L., Yang, W., Lin, Y., 2022. Sulfur isotopic fractionation of the youngest Chang'e-5 basalts: constraints on the magma degassing and geochemical features of the mantle source. Geophys. Res. Lett. 49. https://doi.org/10.1029/2022GL099922
Longhi, J., 1992a. Origin of picritic green glass magmas by polybaric fractional fusion, in: Lunar and Planetary Science Conference Proceedings. pp. 343–353.
Longhi, J., 1992b. Experimental petrology and petrogenesis of mare volcanics. Geochim. Cosmochim. Acta 56, 2235–2251. https://doi.org/10.1016/0016-7037(92)90186-M
McCubbin, F.M., Steele, A., Hauri, E.H., Nekvasil, H., Yamashita, S., Hemley, R.J., 2010. Nominally hydrous magmatism on the Moon. Proc. Natl. Acad. Sci. 107, 11223–11228. https://doi.org/10.1073/pnas.1006677107
Papike, J.J., Vaniman, D.T., 1978. Luna 24 ferrobasalts and the mare basalt suite: comparative chemistry, mineralogy and petrology. Mare Crisium View Luna 24.
Qian, Y., Xiao, L., Wang, Q., Head, J.W., Yang, R., Kang, Y., van der Bogert, C.H., Hiesinger, H., Lai, X., Wang, G., Pang, Y., Zhang, N., Yuan, Y., He, Q., Huang, J., Zhao, J., Wang, J., Zhao, S., 2021. China's Chang'e-5 landing site: geology, stratigraphy, and provenance of materials. Earth Planet. Sci. Lett. 561, 116855. https://doi.org/10.1016/j.epsl.2021.116855
Qian, Y.Q., Xiao, L., Zhao, S.Y., Zhao, J.N., Huang, J., Flahaut, J., Martinot, M., Head, J.W., Hiesinger, H., Wang, G.X., 2018. Geology and scientific significance of the Rümker region in northern Oceanus Procellarum: China's Chang'E-5 landing region. J. Geophys. Res. Planets 123, 1407–1430. https://doi.org/10.1029/2018JE005595
Rhodes, J.M., Blanchard, D.P., Dungan, M.A., Brannon, J.C., Rodgers, K.V., 1977. Chemistry of Apollo 12 mare basalts-Magma types and fractionation processes, in: Lunar and Planetary Science Conference Proceedings. pp. 1305–1338.
Ringwood, A.E., Kesson, S.E., 1976. A dynamic model for mare basalt petrogenesis. Lunar Planet. Sci. Conf. Proc. 7.
Sato, M., Hickling, N.L., McLane, J.W., 1973. Oxygen fugacity values of Apollo 12, 14 and 15 lunar samples and reduced state of lunar magmas. Proc. Fourth Lunar Sci. Conf. Suppl. 4 Geochim. Cosmochim. Acta 1, 1061–1079.

Schmidt, M.W., Kraettli, G., 2022. Experimental crystallization of the lunar magma ocean, initial selenotherm and density stratification, and implications for crust formation, overturn and the bulk silicate Moon composition. J. Geophys. Res. Planets, 127, e2022JE007187.

Shearer, C.K., Hess, P.C., Wieczorek, M.A., Pritchard, M.E., Parmentier, E.M., Borg, L.E., Longhi, J., Elkins-Tanton, L.T., Neal, C.R., Antonenko, I., Canup, R.M., Halliday, A.N., Grove, T.L., Hager, B.H., Lee, D.-C., Wiechert, U., 2006. Thermal and magmatic evolution of the Moon. Rev. Mineral. Geochem. 60, 365–518. https://doi.org/10.2138/rmg.2006.60.4

Singletary, S., Grove, T., 2008. Origin of lunar high-titanium ultramafic glasses: a hybridized source? Earth Planet. Sci. Lett. 268, 182–189. https://doi.org/10.1016/j.epsl.2008.01.019

Snyder, G.A., Taylor, L.A., Neal, C.R., 1992. A chemical model for generating the sources of mare basalts: combined equilibrium and fractional crystallization of the lunar magmasphere. Geochim. Cosmochim. Acta 56, 3809–3823. https://doi.org/10.1016/0016-7037(92)90172-F

Spera, F.J., 1992. Lunar magma transport phenomena. Geochim. Cosmochim. Acta 56, 2253–2265.

Spohn, T., Konrad, W., Breuer, D., Ziethe, R., 2001. The longevity of lunar volcanism: implications of thermal Evolution Calculations with 2D and 3D Mantle Convection Models. Icarus 149, 54–65. https://doi.org/10.1006/icar.2000.6514

Tian, H.-C., Wang, H., Chen, Y., Yang, W., Zhou, Q., Zhang, C., Lin, H.-L., Huang, C., Wu, S.-T., Jia, L.-H., Xu, L., Zhang, D., Li, X.-G., Chang, R., Yang, Y.-H., Xie, L.-W., Zhang, D.-P., Zhang, G.-L., Yang, S.-H., Wu, F.-Y., 2021. Non-KREEP origin for Chang'E-5 basalts in the Procellarum KREEP Terrane. Nature 1–9. https://doi.org/10.1038/s41586-021-04119-5

van Orman, J.A., Grove, T.L., 2000. Origin of lunar high-titanium ultramafic glasses: constraints from phase relations and dissolution kinetics of clinopyroxene-ilmenite cumulates. Meteorit. Planet. Sci. 35, 783–794. https://doi.org/10.1111/j.1945-5100.2000.tb01462.x

Wadhwa M., 2008. Redox conditions on small bodies, the Moon and Mars. Rev. Mineral. Geochem. 68, 493–510.

Wagner, T.P., Grove, T.L., 1997. Experimental constraints on the origin of lunar high-Ti ultramafic glasses. Geochim. Cosmochim. Acta 61, 1315–1327. https://doi.org/10.1016/S0016-7037(96)00387-0

Wieczorek, M.A., Neumann, G.A., Nimmo, F., Kiefer, W.S., Taylor, G.J., Melosh, H.J., Phillips, R.J., Solomo, S.C., Andrews-Hanna, J.C., Asmar, S.W., Konopliv, A.S., Lemoine, F.G., Smith, D.E., Watkins, M.M., Williams, J.G., Zuber, M.T., 2013. The crust of the Moon as Seen by GRAIL. Sci. Rep. 339, 671–675.

Zhang, N., Ding, M., Zhu, M.-H., Li, Huacheng, Li, Haoyuan, Yue, Z., 2022. Lunar compositional asymmetry explained by mantle overturn following the South Pole–Aitken impact. Nat. Geosci. 15, 37–41. https://doi.org/10.1038/s41561-021-00872-4

Zhong, S., Parmentier, E.M., Zuber, M.T., 2000. A dynamic origin for the global asymmetry of lunar mare basalts. Earth Planet. Sci. Lett. 177, 131–140. https://doi.org/10.1016/S0012-821X(00)00041-8

Ziethe, R., Seiferlin, K., Hiesinger, H., 2009. Duration and extent of lunar volcanism: comparison of 3D convection models to mare basalt ages. Planet. Space Sci. 57, 784–796.

Zong, K., Wang, Z., Li, J., He, Q., Li, Y., Becker, H., Zhang, W., Hu, Z., He, T., Cao, K., She, Z., Wu, X., Xiao, L., Liu, Y., 2022. Bulk compositions of the Chang'E-5 lunar soil: insights into chemical homogeneity, exotic addition, and origin of landing site basalts, Geochim. Cosmochim. Acta 335, 284–296,